Compressive strength of thick composite panels

Branner, Kim; Berring, Peter

Published in:
Risoe International Symposium on Materials Science. Proceedings

Publication date:
2011

Document Version
Publisher's PDF, also known as Version of record

COMPRESSIVE STRENGTH OF THICK COMPOSITE PANELS

K. Branner & P. Berring

Wind Energy Division, Risø National Laboratory for Sustainable Energy, Technical University of Denmark, Denmark

ABSTRACT

The aim of this study is to investigate how much the compressive strength of thick composite panels is reduced due to delaminations and to investigate under which conditions a delamination will grow. Understanding of this is essential in order to move forward the design limits used in the structural design process.

Results obtained from finite element modeling analyses are compared with an experimental test campaign performed on flat composite panels with and without delaminations.

1. INTRODUCTION

In wind turbine blades, the flapwise bending loads are typically carried by thick, solid and slightly curved composite panels extending the whole length of the blade. These load-carrying thick laminates are the flanges in the main spar of the blade (see Fig. 1) and experience compressive loading when the blade is bending towards that side. It may therefore be critical when delaminations occur in these load carrying laminates.

In Toft, Branner, Berring and Sørensen (2011) two stochastic models for the distribution of delaminations in wind turbine blades are analyzed. The reliability is estimated for a generic wind turbine blade model both with and without delaminations. It is found that the probability of failure for this particular blade and analysis assumptions increases 5-11 times when delaminations are included.

A panel with a delamination, subjected to compressive loading may buckle and fail in two different ways. The panel may buckle in a local buckling mode, where the sublaminate on mainly one side of the delamination buckles, which typically occurs when the delamination is large in size and positioned close to one of the surfaces. The other buckling mode is global buckling where both the sub-laminate and the remaining panel buckle toward the same side of the panel, which typically occurs when the delamination is small and deep in the laminate. In the local buckling mode, the buckling may drive a growth of the delamination leading to panel

failure (buckling-driven delamination).

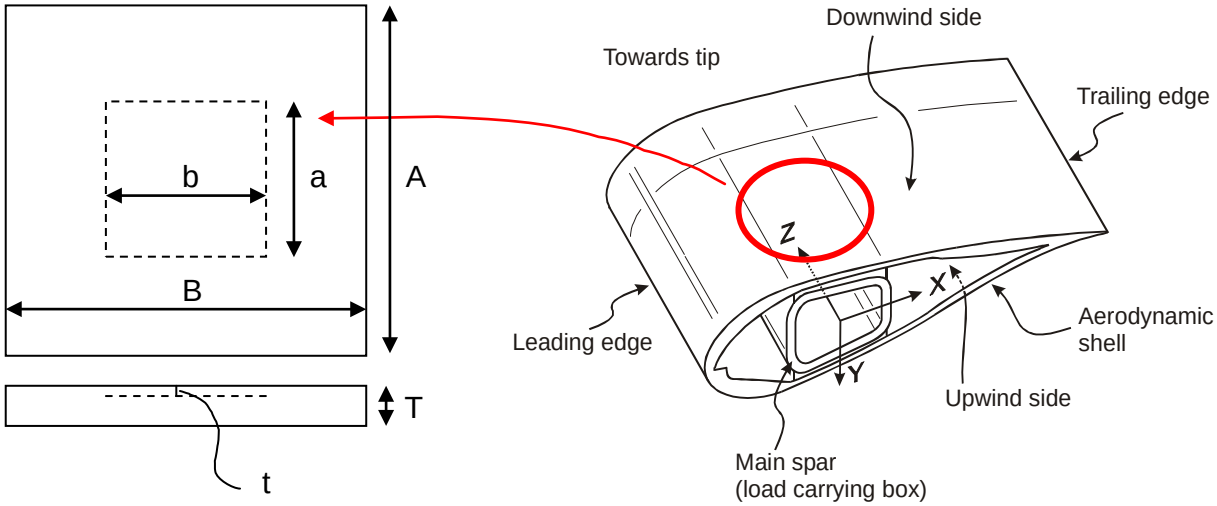

Fig. 1. Definition of panel and delamination geometry. Panels are somewhat similar to the load carrying laminate in the main spar of a typical wind turbine blade.

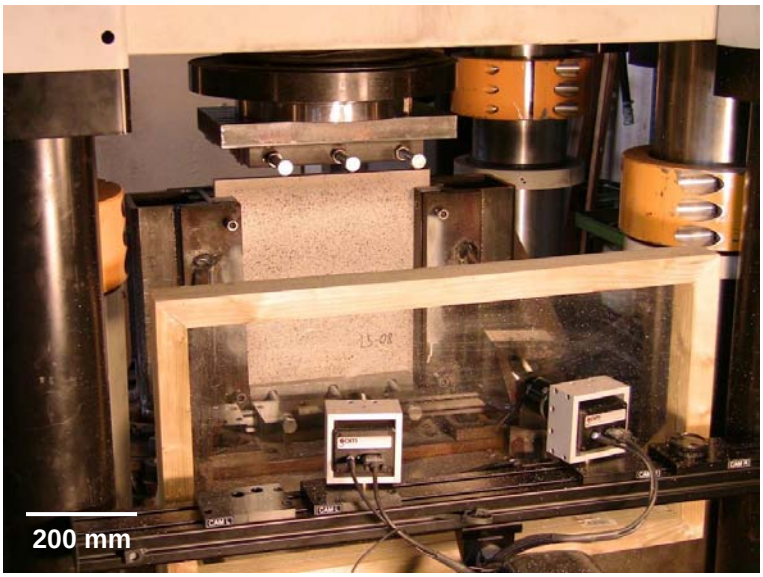

Fig. 2. Panel inserted in the test rig. Note the black speckle pattern on the panel and the two cameras that are used by the digital image correlation (DIC) measurement system to calculate deflections. Scale bar specifies the size of the panel.

2. EXPERIMENTAL RESULTS

A large number of flat composite panels with and without delaminations have been tested until failure as reported in Sørensen, Branner, Lund, Wedel-Heinen and Garm (2009) and Sørensen, Toftegaard, Goutanos, Branner, Berring, Lund, Wedel-Heinen and Garm (2010).

The test specimens are approximately 400x380x20 mm rectangular composite panels made of

glass fiber reinforcement plastic (see Fig. 1). The lay-up is symmetric with approximately 90% of the reinforcement in the load direction and the remaining reinforcement in the ±45º directions. Two different types of panels were tested. One type (PP) was made with prepregs and the other type (VI) was made using the vacuum infusion technique. Even though the specimens were made similar to the load carrying laminate in a typical wind turbine blade, the material properties do not correspond to those in real wind turbine blades, as the specimens were produced in a laboratory under different conditions.

For both types, some of the panels were manufactured with no intentional defects or imperfections, while others had slip sheets embedded to simulate delaminated rectangular areas of a different size and depth. A specially designed test rig (Sørensen et al. 2009) was used in a 5 MN Instron testing machine as shown in Fig. 2. The rig is designed to limit rotation and out-of-plane deflection of the edges of the panels. The panels are supported by steel blocks along the edges on both sides, so the panel area free to experience out-of-plane deflections is approximately 320-325 mm in both the vertical and horizontal direction. The panels were loaded in compression to ultimate failure and a digital image correlation (DIC) measurement system were used on one side of the panel to monitor full field displacements and conventional displacement transducers was used on the other side to monitor the opening of the delamination under the entire load history.

As described above, the compressive loaded panels are subjected to the two different buckling modes; the global buckling mode and the local buckling mode. The following buckling responses were observed during the experiments:

a) Global buckling.

b) Local buckling without growth. The delaminated zone “pops out” and very little growth of the delaminated zone is observed before ultimate failure.

c) Local buckling with growth. The delaminated zone “pops out” and substantial growth of the delaminated zone is observed before ultimate failure.

d) Global buckling with mode jump. The buckling begins in the 1st global mode shape. At failure a mode-jump is observed and the panel fails in an s-shape.

e) Local buckling causes instant failure. The panel fails right after the delaminated zone “pops out”. This typically occurs at high loading.

Table 1 lists the main results from the experimental panel tests. The panels have delaminations of different sizes and through thickness positions (see Fig. 1). For a few of the panels, a strange behavior was observed or measuring equipment was not running properly. These panels are not included here. In Table 1, average results are shown for between 2 and 4 specimens of each type.

2.1 Method to determine buckling load. In Sørensen et al. (2009) a method was developed in order to determine the buckling load. In this method the buckling load was defined as the in-plane load where the tangent to the out-of-plane displacement curve (as a function of the in-plane load) intersects the zero out-of-plane displacement. However, it was found that this method is too sensitive to scatter in the experimental data. In order to ensure consistency for all delamination sizes and through thickness positions, a more robust method for estimating the buckling load proposed in Sørensen et al. (2010) was applied in both the experimental and numerical studies. The normalized in-plane force was plotted vs. the normalized in-plane

displacement. In the beginning of the load history, the response of the panels is linear, but as the panels start to buckle, the response becomes nonlinear.

A linear curve is determined by the first 30% of this load history and then offset by 2.5%. The buckling load is then found as the load at the intersection between this linear curve and a spline interpolation of the entire load history as shown in Fig. 3.

Table 1. List of the tested specimens with delamination sizes and through thickness positions. The prevailing observed buckling modes are listed together with the measured reduced strength, calculated as the average buckling load for that delamination (P_i) relatively to the average buckling load for that type of panel without delamination (P_n).

Test panels					**Failure**	
Code	Specimens	a/A	b/B	t/T	Type	P_i/P_n
VI 2	3	0,33	0,40	0,20	Local	-
VI 3	3	0,25	0,30	0,20	Global	-
VI 4	2		None		Global	100%
VI 5a	3	0,48	0,39	0,31	Global	81%
VI 5b	4	0,47	0,39	0,21	Local	87%
VI 6a	2	0,36	0,30	0,31	Global	87%
VI 6b	4	0,35	0,30	0,21	Local	83%
VI 7a	2	0,42	0,34	0,25	Global	92%
VI 7b	4	0,41	0,34	0,16	Local	82%
PP 1	3	0,52	0,65	0,30	Local?	-
PP 2	3	0,43	0,55	0,35	Local?	-
PP 3	3	0,51	0,65	0,35	Local?	-
PP 5	3		None		Global	100%
PP 6	3	0,82	0,64	0,29	Local	54%
PP 7	3	0,63	0,49	0,29	Local?	63%
PP 8	2	0,68	0,54	0,25	Local?	57%

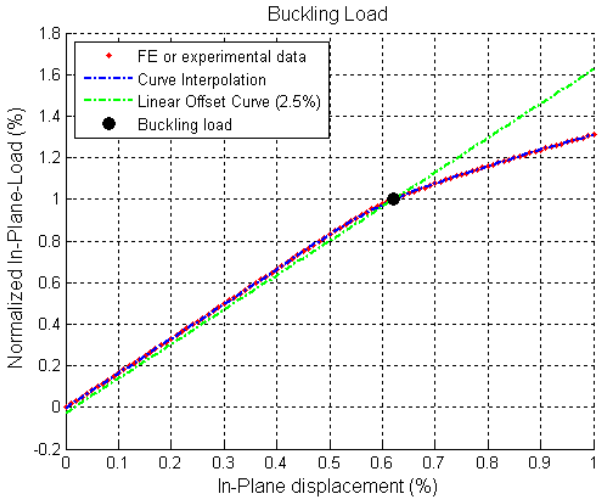

Fig. 3. Robust method to determine the buckling load.

The buckling load was determined for each panel using this robust method. The average buckling loads for the small series of each panel type are denoted P_i and the average buckling loads for panels without delaminations are denoted P_n. The two different series of panels with respect to the manufacturing process were treated separately meaning that they have different P_n. The measured average buckling loads (P_i) with respect to P_n are listed in Table 1.

For some of the early tests the measured buckling loads are not reported in Table 1. These tests were done on an earlier test rig (Sørensen et al. 2009), which has more flexible boundary conditions for the panels. The measured buckling loads are consequently not comparable with those obtained on the newer test rig and therefore not considered here.

3. NUMERICAL MODELING APPROACH

The panels modeled are relatively thick with a thickness to width ratio of about 0.067. They consist entirely of unidirectional (UD) layers with all fibers in the loading direction and are somewhat similar to the load-carrying laminate in a typical wind turbine blade where approximately 90% of the fibers are in the lengthwise direction.

A 3D solid finite-element modeling approach was used with 20-node orthotropic elements. Two or three elements were used through the thickness depending on the through thickness position of the delamination.

A small out-of-plane displacement corresponding to the first buckling mode shape was applied as an initial imperfection of the delaminated sub-laminate. The amplitude of the initial imperfections was approximately 0.5‰ of the panel thickness for the flat panels.

The elements were all joined in the interfaces, except for the delaminated area where quadratic contact conditions were applied to prevent penetration. The panels were simply supported in the midline of all their edges. Therefore, all panel models have nodes at these midlines. The load was applied by forcing a uniform in-place displacement of the short top edge and constraining the opposite edge (B edges in Fig. 1).

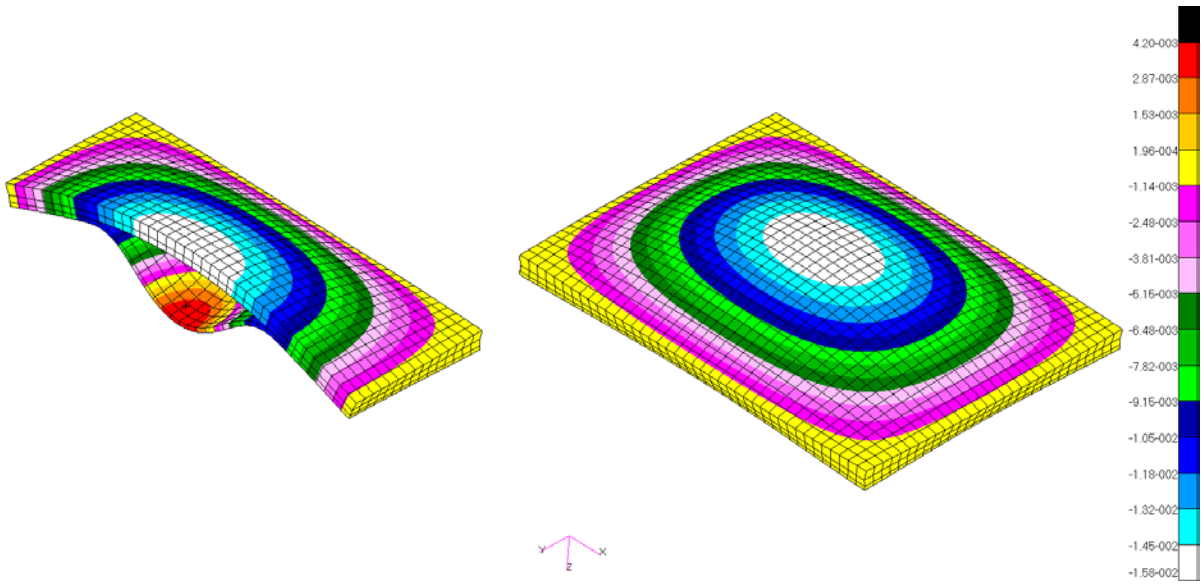

Fig. 4. A typical finite element model showing local buckling behavior.

The average number of degrees of freedom (DOFs) was approximately 150.000. Nonlinear geometric analyses were performed using an implicit solution algorithm and typical results are shown in Fig. 4.

A large numerical parameter study was performed to investigate the buckling response and reduction of strength due to different sizes of delaminations and locations through the thickness of the panels.

In the numerical studies the out-of-plane displacement of two nodes were compared to evaluate which buckling mode the panel had. One node was located at the center of the panel and one node was located at the center of the sub-laminate. In the experimental tests the out-of-plane displacements of the front panel were obtained by applying the DIC measurement system, while the out-of-plane displacement of the back of the panel was measured by applying traditional distance transducers. The displacements of the front and back of the panels were compared to determine if the panel buckled locally (opening of the delamination) or if it buckled globally (no opening of the delamination).

Results from the finite element analyses show that combinations of the global and local modes can also appear as so-called combined modes or sub-modes (see a more detailed description in Sørensen et al. (2009)). The sub-modes occur for large and deep delaminations.

In both the numerical and experimental studies the buckling load of a “perfect” panel was determined based on the robust method described earlier. The reduction of strength resulting from the delamination was determined by performing a normalization based on the results obtained from the “perfect” panels.

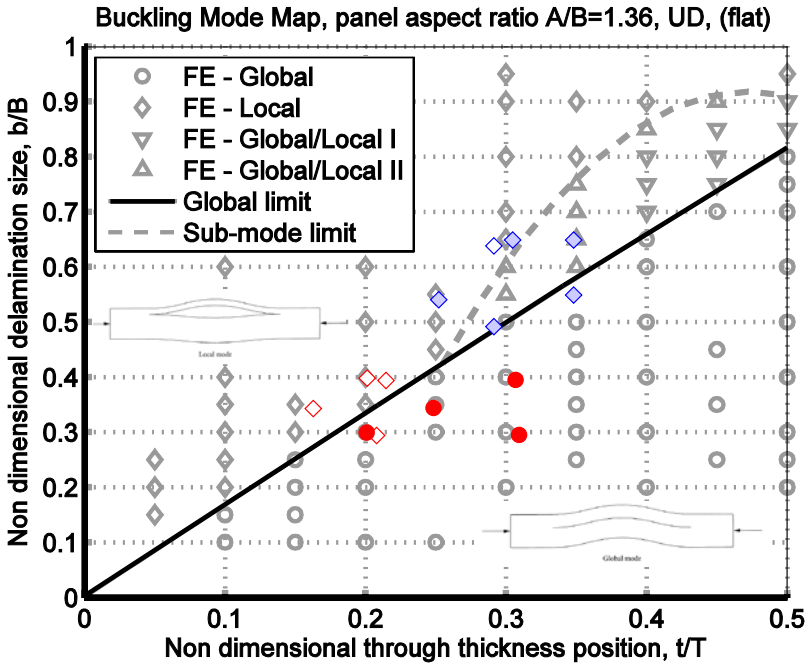

Fig. 5. Buckling mode map for flat UD panels with experimental results included. Type PP panels are blue and type VI panels red. Solid circles mean global buckling while diamonds mean local buckling. The light blue colored diamonds mean that the local behavior is uncertain or the panels sometime show global behavior.

4. COMPARISON

In Fig. 5 the buckling behavior is shown for flat UD panels and compared with the experimental results for the panels tested. It is found that there generally is a good agreement between the predicted buckling behavior and the observed behavior during the experiments. The numerical analyses give a quite sharp borderline between the local and global buckling modes. For the experiments this borderline cannot be expected to be sharp and the experiments also indicate that there is band along the borderline where both local and global buckling behavior can be expected. This band seems to be wider as the delaminations get bigger and deeper in the panels. This also agrees with the sub-mode area found for the numerical analyses. However, more experiments and analyses are needed to obtain more solid conclusions on this band.

The buckling mode map in Fig. 5 is similar to those reported by Short, Guild and Pavier (2001). However, in Short et al. (2001) only local and global modes were considered.

The reduced compressive strength caused by delaminations in the flat UD panels is shown in Fig. 6, where the results from the solid element models are compared with the experimental data. It is generally found that the reduced compressive strength is larger for the experiments than that predicted by the FE-analyses. This is particularly true for the PP type panels, where the strength is reduced more due to delaminations than found for the VI type panels. This may be due to the fact that the experimental and numerical modeled boundary conditions are not the same, but the manufacturing process for the PP type panels may also result in higher sensitivity against delaminations than seen for the VI type panels. More experiments and in-depth analyses are needed in order to make more solid conclusions on the higher observed strength reduction.

In Gaiotti, Rizzo, Branner and Berring (2011) a shell element approach is compared with this solid element approach and in Branner, Berring, Gaiotti and Rizzo (2011) the shell element approach is also compared with these experimental results.

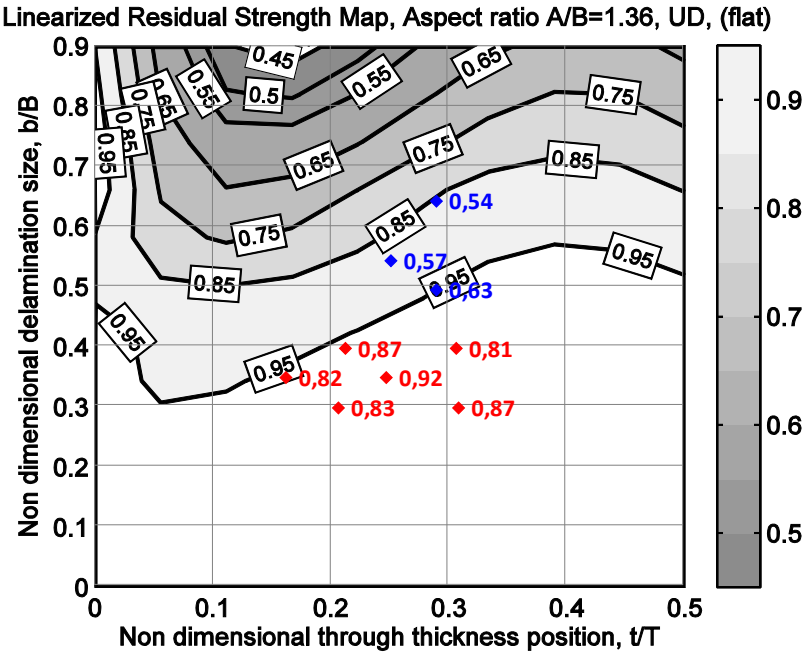

Fig. 6. Reduced compressive strength for flat UD solid element panels with experimental data included. Type PP panels are blue and type VI panels red. The labels indicate the average reduced buckling load factor from the experiments.

5. CONCLUSIONS

Test results from a large number of thick flat composite panels with and without delaminations are presented in this paper and compared with finite element analyses using solid elements. It is found that the compressive strength of thick composite panels is reduced significantly due to delaminations. The reduction of compressive strength is found to be larger for the experiments than predicted by the FE-analyses. This may be due to differences in boundary conditions.

The tests also show that large and deep delaminations caused local buckling and instant failure, while smaller delaminations closer to the surface in some cases are found to give stable delamination growth. When large and deep delaminations open, much elastic energy is released driving a rapid growth of the delamination. These deep delaminations are therefore found to be more dangerous than delaminations closer to the surface where the released elastic energy may not be high enough to drive a growth of the delamination.

ACKNOWLEDGEMENTS

The work is partly supported by the Danish Energy Authority through the 2007 Energy Research Programme (EFP 2007). The supported EFP-project is titled “Improved design of large wind turbine blades of fiber composites – phase 4” and has journal no. 33031-0078.

The work is also partly supported by the Danish Agency for Science, Technology and Innovation through the Danish Centre for Composite Structures and Materials for Wind Turbines (DCCSM) (project no. 09-067212). The support is gratefully acknowledged.

REFERENCES

Branner, K., Berring, P., Gaiotti M. and Rizzo, C.M. (2011) Comparison of Two Finite Element Methods with Experiments of Delaminated Composite Panels, in: Proc. of 18th International Conference of Composite Materials (ICCM), 21-26 August 2011, Jeju Island, Korea.

Gaiotti, M., Rizzo, C.M., Branner K. and Berring, P. (2011). Finite Elements Modeling of Delaminations in Composite Laminates, in: Proc. of 3rd International Conference on Marine Structures (MARSTRUCT), 28-30 March 2011, Hamburg, Germany.

Short, G.J., Guild F.J. and Pavier. M.J. (2001) The effect of delamination geometry on the compressive failure of composite laminates, Composites Science & Technology, 61, 2075-2086.

Sørensen, B.F., Branner, K., Lund, E., Wedel-Heinen J. and Garm. J.H. (2009). Improved design of large wind turbine blade of fibre composites (phase 3). Summary Report, Risø-R-1699(EN), Risø National Laboratory for Sustainable Energy, Denmark.

Sørensen, B.F., Toftegaard, H., Goutanos, S., Branner, K., Berring, P., Lund, E., Wedel-Heinen J. and Garm. J.H. (2010). Improved design of large wind turbine blade of fibre composites (phase 4). Summary Report, Risø-R-1734(EN), Risø National Laboratory for Sustainable Energy, Denmark.

Toft, H.S., Branner, K., Berring P. and Sørensen, J.D. (2011). Defect Distribution and Reliability Assessment of Wind Turbine Blades, Engineering Structures, 33(1), 171-180, DOI: 10.1016/j.engstruct.2010.10.002.